Multi-channel intramuscular and surface EMG decomposition by convolutive blind source separation

2016 J. Neural Eng. 13 026027

(http://iopscience.iop.org/1741-2552/13/2/026027)

IOP Publishing Journal of Neural Engineering
J. Neural Eng. 13 (2016) 026027 (17pp) doi:10.1088/1741-2560/13/2/026027

Multi-channel intramuscular and surface EMG decomposition by convolutive blind source separation

Francesco Negro[1], Silvia Muceli[1], Anna Margherita Castronovo[1], Ales Holobar[2] and Dario Farina[1]

[1] Institute of Neurorehabilitation Systems, Bernstein Focus Neurotechnology Göttingen, Bernstein Center for Computational Neuroscience, University Medical Center Göttingen, Georg-August University of Göttingen, Göttingen, Germany
[2] Faculty of Electrical Engineering and Computer Science, University of Maribor, Maribor, Slovenia

E-mail: dario.farina@bccn.uni-goettingen.de

Received 24 July 2015, revised 1 December 2015
Accepted for publication 27 January 2016
Published 29 February 2016

Abstract

Objective. The study of motor unit behavior has been classically performed by selective recording systems of muscle electrical activity (EMG signals) and decomposition algorithms able to discriminate between individual motor unit action potentials from multi-unit signals. In this study, we provide a general framework for the decomposition of multi-channel intramuscular and surface EMG signals and we extensively validate this approach with experimental recordings. *Approach.* First, we describe the conditions under which the assumptions of the convolutive blind separation model are satisfied. Second, we propose an approach of convolutive sphering of the observations followed by an iterative extraction of the sources. This approach is then validated using intramuscular signals recorded by novel multi-channel thin-film electrodes on the Abductor Digiti Minimi of the hand and Tibilias Anterior muscles, as well as on high-density surface EMG signals recorded by electrode grids on the First Dorsal Interosseous muscle. The validation was based on the comparison with the gold standard of manual decomposition (for intramuscular recordings) and on the two-source method (for comparison of intramuscular and surface EMG recordings) for the three human muscles and contraction forces of up to 90% MVC. *Main results.* The average number of common sources identified for the validation was 14 $\pm$ 7 (averaged across all trials and subjects and all comparisons), with a rate of agreement in their discharge timings of 92.8 $\pm$ 3.2%. The average Decomposability Index, calculated on the automatic decomposed signals, was 16.0 $\pm$ 2.2 (7.3–44.1). For comparison, the same index calculated on the manual decomposed signals was 15.0 $\pm$ 3.0 (6.3–76.6). *Significance.* These results show that the method provides a solid framework for the decomposition of multi-channel invasive and non-invasive EMG signals that allows the study of the behavior of a large number of concurrently active motor units.

Keywords: EMG, motor unit, motor neuron, decomposition, blind source separation

(Some figures may appear in colour only in the online journal)

Introduction

Since the pioneering work of Adrian and Bronk (Adrian and Bronk 1929), the recording of the discharge timings of motor units during voluntary contractions has provided a fundamental knowledge to our understanding of human movement (Heckman and Enoka 2004, 2012). The access to motor units can occur via recording of the muscle fiber action potentials since the neuro-muscular junction is a highly reliable synaptic connection (Enoka 2008). Each discharge of a

motor neuron systematically corresponds to muscle fiber action potentials in the innervated muscle unit. The motor unit discharge timings therefore reflect the corresponding motor neuron discharge pattern. In this way, the analysis of motor units provides a window into the activity of the output layer of the spinal circuitries.

For several decades following the introduction of the concentric needle (Adrian and Bronk 1929), the study of motor units has been performed by invasive technologies (Merletti and Parker 2004, Merletti and Farina 2009) based on wire or needle electrodes. From the signal processing point of view, the identification of single motor unit activity from the multi-unit needle/wire recordings has been assisted by (semi) automatic algorithms for EMG decomposition whose performance improved substantially over the last decade (McGill *et al* 2005, Florestal *et al* 2006, Florestal *et al* 2007, Nawab *et al* 2008, Merletti and Farina 2009, Ge *et al* 2010, Ge *et al* 2011, Marateb *et al* 2011b). Despite their relevance, these approaches have nonetheless limited our view on motor unit behavior to a relatively small sample of motor units concurrently identified and to relatively low contraction forces (Farina *et al* 2014, Farina and Negro 2015). These limits derive from the need for selective recordings and from the difficulty of classic decomposition algorithms to deal with many sources overlapping in time. In recent times, alternative approaches have been proposed for solving the limitations of the classic methods for motor unit investigations. The main trend has been the development of multi-channel recording systems for EMG detection, both invasive (Farina *et al* 2008b, Muceli *et al* 2015) and non-invasive (Merletti and Parker 2004).

Invasive multi-channel recordings have been introduced with the rationale that the spatial sampling of the muscle cross-section would increase the number of identified units, still maintaining high selectivity for each detection site (Farina *et al* 2008b). Recently, a thin-film wire electrode system with closely spaced electrodes (high-density) for human recordings has been designed and extensively tested (Muceli *et al* 2015). Concurrently, surface EMG technology, which inherently has poorer selectivity than invasive methods, has been extended in the last two decades from single bipolar derivations to multi-channel systems (high-density) comprising up to hundreds of electrodes, with the aim of discriminating single motor unit activity using the spatial representation of their action potentials (Merletti and Parker 2004, Farina *et al* 2008a).

The availability of multi-channel (>10 channels) intramuscular and surface EMG technologies has opened a new research scenario in the development of algorithms for EMG decomposition. Indeed, by increasing the number of channels to tens or even hundreds, it is now possible to apply latent component analysis approaches, which usually require multiple EMG signal observations to identify motor unit activities. This approach has been used first in the Convolution Kernel Compensation (CKC) algorithm for high-density surface EMG decomposition (Holobar and Zazula 2007a, Holobar and Zazula 2007b, Holobar *et al* 2010) and, later on, by other algorithms (Liu *et al* 2014, Ning *et al* 2014, Chen and Zhou 2015). Conversely, these approaches have not yet been applied to multi-channel invasive EMG, mainly because the technology for these recordings has been made available for human recordings only very recently (Farina *et al* 2008b, Muceli *et al* 2015).

In this paper, we present (i) a general framework for multi-channel EMG (surface or intramuscular) decomposition by combining approaches based on convolutive blind source separation (Holobar and Zazula 2007a, Holobar and Zazula 2007b, Negro *et al* 2009, Holobar *et al* 2010, Chen and Zhou 2015), and (ii) a systematic experimental validation of this framework in different muscles with the two source approach (Holobar *et al* 2010, Holobar *et al* 2014). The framework for decomposition contains, as special cases, the methods presented in (Holobar and Zazula 2007a, Holobar and Zazula 2007b, Ning *et al* 2014, Chen and Zhou 2015). In addition to applying this decomposition approach to surface EMG, as done in (Holobar *et al* 2010, Holobar *et al* 2014, Ning *et al* 2014, Chen and Zhou 2015), we show for the first time the fully automatic decomposition of novel multi-channel invasive wire recordings (Farina *et al* 2008b, Muceli *et al* 2015). Finally, since the validation is a key step in proposing new techniques for EMG decomposition (Farina and Enoka 2011, Farina *et al* 2014, 2015, Holobar *et al* 2014, De Luca *et al* 2015), we present a solid experimental validation of the decomposition results, both with reference to the gold standard of full manual decomposition by experts (for invasive recordings) and with the conservative measure of accuracy provided by variations of the two-source method (Mambrito and De Luca 1984, De Luca *et al* 2006, Holobar *et al* 2010, Marateb *et al* 2011a, Hu *et al* 2014). Summarizing, the paper provides a general framework for the decomposition of multi-channel invasive and non-invasive EMG signals as well as a solid validation of the approach.

Materials & methods

Theory and algorithm

Multi-channel EMG signals, either invasively or non-invasively recorded, share the same generation model and can be described as a convolutive mixture of a series of delta functions, representing the discharge timings of the motor units (Holobar and Zazula 2007a, Holobar and Zazula 2007b, Holobar *et al* 2010). The impulse responses of the filters in this convolutive mixture are the action potentials of the muscle units, which have finite duration (Holobar and Zazula 2007a, Holobar and Zazula 2007b):

$$x_i(k) = \sum_{l=0}^{L-1}\sum_{j=1}^{n} h_{ij}(l)s_j(k-l) + n_i(k), \qquad (1)$$

$$i = 1,\ldots,m \; k = 0,\ldots,D_R$$

where $x_i(k)$ is the ith EMG channel, k is the discrete time, D_R is the duration of the recording (in samples), $h_{ij}(l)$ the action potential of the jth motor unit as recorded at the channel i, $s_j(k)$ the spike train of the jth motor unit, $n_i(k)$ the additive

noise at channel i, L the duration of the action potentials, and n and m the number of active motor units and channels (observations), respectively. In matrix form, equation (1) becomes:

$$\underline{x}(k) = \sum_{l=0}^{L-1} \underline{\underline{H}}(l)\,\underline{s}(k-l) + \underline{n}(k) \tag{2}$$

where $\underline{x}(k) = [x_1(k), x_2(k), ..., x_m(k)]^T$ and $\underline{s}(k) = [s_1(k), s_2(k), ..., s_n(k)]^T$ are the vectors comprising the k-th sample of m EMG signals recorded in/on the muscle and the n motor unit spike trains (sources) that generate the EMG signals, respectively. This model is valid for any multi-channel EMG recording, invasive or non-invasive. Therefore, in the following we will treat the problem of EMG decomposition in general.

For each sample l, the matrix $\underline{\underline{H}}(l)$ is of size $m \times n$, whereas l ranges from 0 to L-1. The matrix of action potentials is assumed to be constant for the duration D_R of the analyzed signal. From the recorded signals $\underline{x}(k)$, the aim is to identify the largest number of sources of the matrix $\underline{s}(k)$. For this estimate, we assume that the identified sources are not fully correlated and either independent or sparse (Holobar and Farina 2014, Farina and Holobar 2015). The non-identified sources are modelled into the additive noise term in equation (2).

A convolutive mixture with finite impulse response filters, as in equation (2), can be represented as a linear and an instantaneous mixture of an extended vector of sources that include the original sources and their L-1 delayed versions (Holobar and Zazula 2007a, Holobar and Zazula 2007b). The new source vector after the extension has size $nL \times 1$. In order to increase the ratio between the number of observations and the number of sources and, thus, conditionality of the described mixing process, the observations are also usually extended, adding R delayed versions of each observation. This leads to the following extended observation vector for channel i (Holobar and Zazula 2007a, Holobar and Zazula 2007b, Holobar *et al* 2010):

$$\tilde{x}_i(k) = [x_i(k)x_i(k-1), \ldots, x_i(k-R)]\ i = 1, \ldots, m$$

After the extension of the observations, we also have:

$$\tilde{s}_j(k) = [s_j(k), s_j(k-1), \ldots, s_j(k-L-R+1)]$$
$$j = 1, \ldots, n$$

and

$$\tilde{n}_i(k) = [n_i(k), n_i(k-1), \ldots, n_i(k-R)]\ i = 1, \ldots, m$$

Therefore, we can define the extended model as (Holobar and Zazula 2007a, Holobar and Zazula 2007b, Holobar *et al* 2010):

$$\underline{\tilde{x}}(k) = \underline{\underline{\tilde{H}}}\,\underline{\tilde{s}}(k) + \underline{\tilde{n}}(k) \quad k = 0, \ldots, D_R \tag{3}$$

with

$$\underline{\tilde{s}}(k) = [\tilde{s}_1(k), \tilde{s}_2(k), \ldots, \tilde{s}_n(k)]^T$$
$$\underline{\tilde{x}}(k) = [\tilde{x}_1(k), \tilde{x}_2(k), \ldots, \tilde{x}_m(k)]^T$$
$$\underline{\tilde{n}}(k) = [\tilde{n}_1(k), \tilde{n}_2(k), \ldots, \tilde{n}_m(k)]^T$$

$$\tilde{h}_{ij} = \begin{bmatrix} h_{ij}[0] & \cdots & h_{ij}[L-1] & 0 & \cdots & 0 \\ 0 & \ddots & \ddots & \ddots & \ddots & \vdots \\ \vdots & \ddots & \ddots & \ddots & \ddots & 0 \\ 0 & \cdots & 0 & h_{ij}[0] & \cdots & h_{ij}[L-1] \end{bmatrix}$$

$$\underline{\underline{\tilde{H}}} = \begin{bmatrix} \tilde{h}_{11} & \cdots & \tilde{h}_{1n} \\ \vdots & \ddots & \vdots \\ \tilde{h}_{m1} & \cdots & \tilde{h}_{mn} \end{bmatrix}$$

In order to solve the inverse problem, the number of extended measurements should be higher than the number of sources multiplied by the length of the filters (MUAP shapes). If this assumption is satisfied, equation (3) defines an over-determined system that can be solved by using an ordinary least square methods if the matrix H is full rank. In this study, we used an extension factor $R = 1000/m$. We tested different values of the extension parameter, but the results for the iEMG signals were not substantially influenced by this parameter for values higher than 16 (see Results section).

In general, the product between the extension factor and the number of available channels should be approximately equal or greater than the number of sources multiplied by the duration of the MUAPs. In other words, $R \geqslant (n/m)L$, where L is the length of the MUAPs in samples. Therefore, relatively long MUAP shapes require large extension factors unless the number of recorded channels is high. In our study, the MUAP shapes identified in the iEMG signals were substantially shorter than the ones commonly recorded when using sEMG electrodes. Therefore, the selected value of extension factor was a trade-off between the assumption previously explained, the number of extracted sources, and the average accuracy.

Since the first step of the proposed algorithm is the whitening for time lag zero, it is important that the extended sources maintain the property of uncorrelation at least for time lag zero, i.e. $\underline{\underline{R}}_{\tilde{s}_i\tilde{s}_i}(0)$ is diagonal. This property is intrinsic to point sources with refractory period, as it has been previously shown (Holobar and Zazula 2007b) and as also reported, with the notations of the present paper, in the appendix for completeness. These conditions are very well approximated for the statistics of motor unit discharges. Therefore, the new sources made of the delayed original sources remain approximately uncorrelated whenever the original sources are uncorrelated.

Classic approaches of blind separation build on the independency of the sources. We note, however, that the extended spike trains in equation (3) are never independent. Nonetheless, the contrast functions used for source separation in blind source sepearation algorithms also measure the sparseness of the sources (motor unit spike trains). Contrary

to independence, the sparseness property is also maintained after extension of the sources because of the specific structure of the sources as spike trains (most samples are zero). Intuitively, this is due to the fact that the summation of sources with correlated firings is always less sparse than the individual sources, unless the firings are fully coincident (Farina and Holobar 2015). Therefore, the idea that common drive and short-term synchronization between motor unit spike trains may violate the *foundational mathematical assumptions* of the blind source separation techniques applied to multi-channel EMG signals (Nawab *et al* 2008) does not hold for point processes. Because of the specific characteristics of the spike trains generated by motor units, the linear instantaneous mixture model in equation (3), obtained as the extension of the convolutive mixture model of multi-channel EMG signals, maintains the properties required by the proposed source separation algorithm (Farina and Holobar 2015). The blind source separation problem is therefore simplified to un-mixing a linear, instantaneous mixture of *sparse* sources [see equation (3)].

In this study, we solve the separation problem for the model in equation (3) by combining the approaches proposed in (Thomas *et al* 2006) (general approach to blind separation without specific applications), (Chen and Zhou 2015) (separation of surface EMG by fast independent component analysis, fastICA), and (Holobar and Zazula 2007a, Holobar and Zazula 2007b, Holobar *et al* 2010) (CKC decomposition of surface EMG signals).

The first step of our approach is common to many general-purpose blind source separation methods, e.g., SOBI (Belouchrani *et al* 1997), and includes spatial whitening of the extended observations. The combination of the extension procedure described above and the whitening has also been referred to as 'convolutive sphering' (Thomas *et al* 2006). A whitening matrix W is obtained by imposing that the whitened extended observation matrix

$$\underline{z}(k) = \underline{\underline{W}}\,\underline{\tilde{x}}(k) \tag{4}$$

has a covariance matrix equal to the identity for time lag zero. By imposing this condition, the whitening matrix is obtained as:

$$\underline{\underline{W}} = \underline{\underline{U}}\,\underline{\underline{D}}_S^{\gamma}\,\underline{\underline{U}}^T \tag{5}$$

with $\gamma = -1/2$, and where $\underline{\underline{U}}$ is the diagonalization matrix of the covariance matrix of the extended observations (obtained for example by its eigenvalue decomposition):

$$\underline{\underline{R}}_{\tilde{x}\tilde{x}} = \underline{\underline{U}}\,\underline{\underline{D}}_S\,\underline{\underline{U}}^T \text{ with } \underline{\underline{R}}_{\tilde{x}\tilde{x}} = E\{\underline{\tilde{x}}(k)\,\underline{\tilde{x}}^T(k)\} \tag{6}$$

This eigenvalue decomposition is possible because of the uncorrelation of the extended sources for time lag zero (see appendix). The eigenvalue decomposition has been performed in this study with a regularization factor fixed for all recordings to the average of the smallest half of the eigenvalues of the correlation matrix of the extended EMG signals. The regularization procedure was applied to reduce the numerical instability of the solutions of the inverse problem. In this study, the selected regularization factor was equivalent to assuming the noise variance equals to the average of the smallest half of the eigenvalues (Belouchrani *et al* 1997). In general, the selection of the regularization factor is not trivial. The selection of low values may preserve part of the noise components and influence the estimated sources. At the same time, the selection of high values may influence the sources with relatively low amplitude that would be discarded by the subsequent estimation process. The sources can be retrieved after whitening by finding the correction rotation (unitary) matrix to transform the whitened observations into the estimated sources. This matrix can be obtained, for example, as the matrix of eigenvectors of the autocorrelation matrix of the extended and whitened observations for time lags different from zero (Belouchrani *et al* 1997, Belouchrani and Amin 1998). This close solution, which requires only the uncorrelation of the sources, however, becomes impractical (for computational reason) when the number of original sources is large. We therefore applied the fixed-point algorithm (Hyvärinen and Oja 1997), as used in (Thomas *et al* 2006), with a Gram–Schmidt orthogonalization step to increase the number of unique sources that are estimated (Hyvärinen and Oja 2000). After this iteration, the motor unit spike train is estimated by a peak detection algorithm applied to the squared of the source vector (Holobar and Zazula 2007a, Holobar and Zazula 2007b, Holobar *et al* 2010) and K-means classification (two classes) of the identified peaks. For the latter step, the K-means++ algorithm was used (Arthur and Vassilvitskii 2007). The class with the highest centroid was selected for the estimation of the discharge times. In the proposed study, in most cases, the source vector contained the contribution of relatively high peaks (A) and relatively small peaks (B). The high peaks corresponded to the firing occurrences of one motor unit only while small peaks were generated by one or more motor units. We used a two class algorithm to separate A from B, without separating the motor units that contributed to B. This implies the loss of the motor units constituting B, unless they appeared in a different source vector or they have been improved by the next iterative procedure. In fact, we included a second iterative procedure to improve the estimation of the motor unit discharge trains by adding a loose constraint to the solution. This second iteration is derived from the CKC approach and is important since the fixed point algorithm may converge to unreliable estimates (Wei 2014). This iteration consists in improving the estimate with the separation vector calculated from the estimated discharge timings, until reaching a minimum in the variability of discharge. This assumption favors the regularity of the discharges, as a desirable characteristics of the sources (although it does not force the estimates to be regular). The same assumption has been made in different approaches for intramuscular EMG decomposition (e.g., (Monsifrot *et al* 2011)).

Finally, a silhouette measure (SIL) was computed on the estimated source after the second iteration and the source was automatically selected as of acceptable quality if SIL was greater than a threshold (TH_{SIL}), set to 0.90 in the current study. The SIL was defined as the difference between the within-cluster sums of point-to-centroid distances and the

same measure calculated between clusters. The measure was normalized dividing by the maximum of the two values. Although with a different definition, the measure SIL provides an index of reliability similar to the pulse to noise ratio (PNR) defined in (Holobar *et al* 2014), but, since SIL is a normalized measure, it can be directly associated to the estimated rate of agreement (RoA, see Results).

The overall algorithm is summarized in the pseudo-code, where w_i is the i-th separation vector and $g(x)$ is the first derivative of a general contrast function $G(x)$ ($\mathrm{d}G(x)/\mathrm{d}x = g(x)$) that measures the sparseness of the sources, $\boldsymbol{B}$ is the separation matrix whose columns are the separation vectors w_i, and n is the iteration number. The fixed point algorithm is used to find the separation vector w_i for the ith source. Originally, the fastICA's contrast functions were designed to maximize the non-Gaussianity and, indirectly, the independence of the estimated sources ${w_i}^T\mathbf{z}$. In our case, the sources are supergaussian, i.e. sparse, thus the contrast functions $G(x)$ are used as measures of sparseness rather than measures of independence. As discussed above and demonstrated in the Results section, this leads to full separation of the extended sources, even though the extended sources are not independent. Indeed, the summation of sources is always less sparse that the individual sources, even if some firings are synchronized. This property is always valid unless all firings are exactly synchronized. It is worth noting that for this second step, neither the uncorrelation nor the independence of the extended sources is required. Therefore, the full algorithm requires only uncorrelation of the extended sources for time lag zero (whitening, see also appendix) and sparseness of the sources which is an intrinsic property of spike trains.

In general, a fast convergence of the fixed point algorithm, as in other algorithms (Holobar and Zazula 2007a), requires a suitable initialization point of the projection vector. In this study, a different initialization step was used compared to (Thomas *et al* 2006). For each new source to be estimated, the time instant corresponding to the maximum of the squared summation of all whitened extended observation vector was located and then the projection vector was initialized to the whitened observation vector at the same time instant. The rationale for this choice is that the time instant of the observation vectors with highest activity is likely to belong to one or more motor unit discharges at that time instant. This initialization follows the same rationale as the 'activity index' in (Holobar and Zazula 2007a, Holobar and Zazula 2007b).

- Subtract the mean from the observations $\underline{\tilde{x}}$
- Whiten $\underline{\tilde{x}}$
- Initialize the matrix $\underline{\underline{B}}$ to empty matrix
- For $i = 1, 2, \ldots, M$ repeat:
  1. Initialize the vector $w_i(0)$ and $w_i(-1)$
  2. While $|w_i(n)^T w_i(n-1) - 1| \prec Tolx$
     a. Fixed Point Algorithm:

$$w_i(n) = E\{\underline{z}g[w_i(n-1)^T\underline{z}]\} - Aw_i(n-1)$$

with $A = E\{g'[w_i(n-1)^T\underline{z}]\}$

b. Orthogonalization

$$w_i(n) = w_i(n) - \underline{\underline{B}}\underline{\underline{B}}^T w_i(n)$$

c. Normalization

$$w_i(n) = \frac{w_i(n)}{\|w_i(n)\|}$$

d. Set $n = n + 1$

  3. End while
  4. Initialize CoV_{n-1} and CoV_n
  5. While $CoV_n < CoV_{n-1}$
     a. Estimate the i-th source

$$\hat{s}_i(k) = w_i(n)^T\underline{z}(k)$$

     b. Estimate the pulse train PT_n with peak detection and K-means classification
     c. Set $CoV_{n-1} = CoV_n$ and calculate CoV_n of PT_n
     d. $w_i(n+1) = \frac{1}{J}\sum_{j=1}^{J}\underline{z}(t_j)$
        with $t_j = \{t: PT_n(t) = 1\}$ denoting a set of J pulses in PT_n
     e. Set $n = n + 1$
        End While $\mathrm{CoV}_n < \mathrm{CoV}_{n-1}$
  6. if SIL > 0.9
     a. Accept the source estimate
     b. Add w_i to the matrix $\underline{\underline{B}}$
- End For Loop

Assuming $A = -1$ and g a suitable update function, the first iteration of the proposed algorithm is similar to the method referred to as gradient CKC (gCKC) approach (Holobar and Zazula 2007a, Holobar and Zazula 2007b). However, the gCKC approach uses a gradient based optimization that has different convergence properties than the fixed point algorithm. Without the second iteration, on the other hand, the proposed algorithm corresponds to the fast ICA implementation (Hyvärinen and Oja 1997). The second iteration follows the steps proposed in the CKC algorithm (Holobar and Zazula 2007b) to further refine the source estimates. Figure 1 shows a representative example of the algorithm applied to a synthetic signal. Three synthetic sources were mixed in three signals. For clarity and graphical purposes, we showed the steps with an extension factor equal to 9. However, we performed the extraction using an extension factor of 30. In fact, the MUAP shapes were 9 samples long, therefore we selected an extension factor higher than 3 sources x 9 samples.

In the fast ICA framework, the estimated sources are often subtracted from the observations (peel-off approach), as in (Chen and Zhou 2015). This operation was also performed in (Hyvärinen and Oja 2000, Thomas *et al* 2006) and serves to increase the number of estimated sources, which, without further processing, would be very small. However, we note that, for the decomposition of multi-channel EMG signals (especially intramuscular signals, with smaller duration of the action potentials), the subtraction of the estimated sources

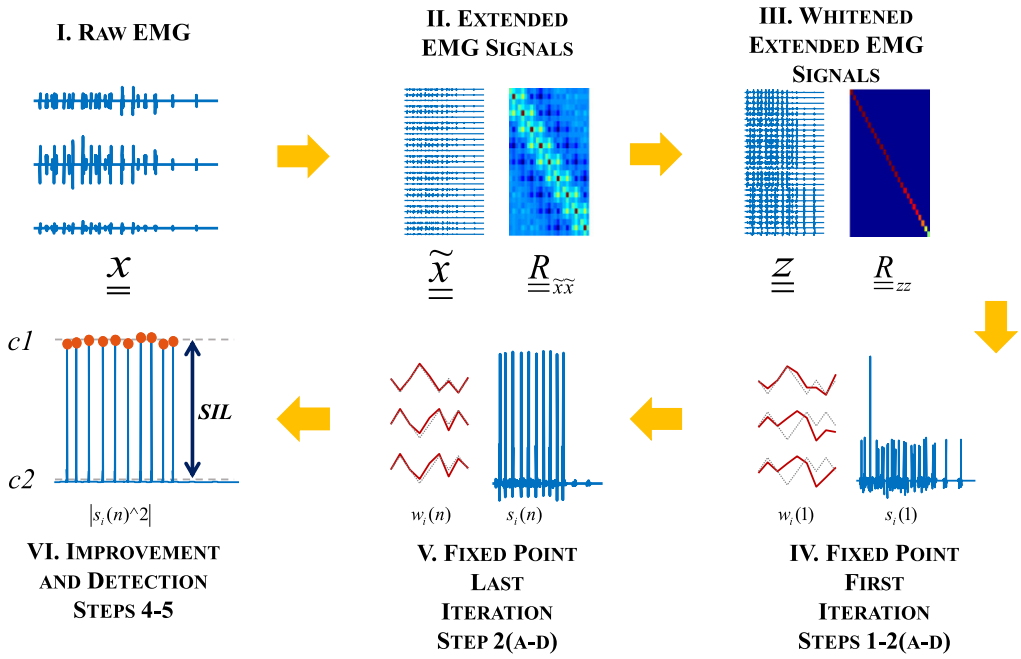

Figure 1. Representative example of the working principles of the algorithm on a synthetic signal. Three synthetic sources were mixed in three observations. The synthetic MUAP shapes had a duration of 9 samples. Therefore, for clarity and graphical purposes, we show the steps of the algorithm with an extension factor equal to 9. However, we performed the calculation using an actual extension factor of 30 (>3 sources x 9 samples). (I) Raw synthetic EMG mixture. (II) Extended EMG measurements (left) and the corresponding correlation matrix (right). (III) Whitened extended EMG measurements (left) and corresponding correlation matrix (approximately diagonal) (right). (IV) Projection vector (left) and the estimated source (right) after the first step of the fixed point algorithm. (V) Projection vector (left) and the estimated source (right) after the last step of the fixed point algorithm. (VI) Improvement of the estimation (see figure 3 for details) and calculation of the SIL measure. The SIL is a normalized measure of the distance between the clusters of the detected points (c1) and the cluster of the noise values (c2).

may not be the optimal choice. Indeed, at each iteration in which an estimated source is subtracted, the residual signal contains a noise component that increases with the number of subtractions. This is due to alignment errors in the subtraction procedure, which are unavoidable. To avoid the problems inherent in a peel-off approach, we used a source deflation procedure (the orthogonalization step 2.b in the pseudo code) (Hyvärinen and Oja 2000) that favors the estimation of different sources at each completed iteration. The proposed orthogonalization has limitations compared with the 'symmetric orthogonalization' (Hyvarinen 1999, Ollila 2010), but it is superior in terms of computational complexity.

In the results presented in this study, different contrast functions have been tested, ranging from the skewness $G(x) = x^3/3$ (Hyvarinen 1999, Mitianoudis *et al* 2005), to functions more robust to outliers, such as $G(x) = \log(\cosh(x))$ and $G(x) = \exp(-x^2/2)$, suggested for the fastICA algorithm. The skewness function offers very fast convergence, but is also sensitive to outliers and signal artifacts and, thus, less appropriate when the EMG signals are of poor recording quality. However, this problem is mitigated by the orthogonalization step that avoids the multiple convergences to the same 'artifact based' solution.

In conclusion, the proposed algorithm (see pseudo-code) is a combination of approaches for source separation, each chosen with rigorous theoretical rationales, with modifications adopted for optimizing each step for the specific application of EMG signal decomposition. The resulting approach is a new method for EMG decomposition that can be applied to both intramuscular and surface multi-channel signals. The two main iterations of this approach are based on a fastICA separation vector (with sparse, and not independent, sources) and a source estimation refinement step based on the CKC approach. Since validation is essential, this study reports a complete validation of accuracy of the method on experimental signals.

Evaluation of accuracy

The proper procedure for validation of EMG decomposition is still an open and highly debated problem (Farina and Enoka 2011, Farina *et al* 2014, 2015, Holobar *et al* 2014, Kline and De Luca 2014, De Luca *et al* 2015). Although simulated signals may be the first means for validation, the final proof of the appropriateness of the proposed method should be based on experimental recordings. In this study, we do not show simulation results, for the sake of brevity, although simulations have been extensively used as a first validation step. Rather, we focus on the experimental validation for both intramuscular and surface EMG signals. For intramuscular signals, the decomposition accuracy can be estimated by comparing the automatic decomposition with a carefully performed manual decomposition by one or more experts. This approach will also be presented in this study. Nonetheless, this method is not applicable when a manual decomposition cannot be obtained, e.g. with surface EMG.

Currently, the only sufficiently validated method for testing the accuracy of EMG decomposition in the absence of a gold standard provided by expert decomposition, is the comparison of the decomposition results of two or more EMG signal sets that share some common sources (discharge timings) (De Luca *et al* 2006, Holobar *et al* 2010, Holobar and Farina 2014), but also have a number of different sources and different action potential shapes. In these conditions, when the two decompositions agree, they are assumed as correct since making the exact same errors in decomposing two almost independent recordings is very unlikely. We will refer to this method of validation as the two source method (Mambrito and De Luca 1984). According to this method, the RoA between the decompositions is used as a conservative estimate of accuracy:

$$RoA = \frac{c_j}{c_j + A_j + B_j} \cdot 100\% \quad (7)$$

where c_j is the number of discharges of the jth motor unit spike train that was identified by both decompositions (tolerance in discharge timing $\pm$ 0.5 ms), A_j the number of discharges identified only by one of the two decompositions, and B_j the number of discharges identified only by the other decomposition. Two motor unit discharge patterns were considered as generated by the same motor unit if c_j corresponded to more than 30% (Holobar and Zazula 2007b). Discharge patters with coefficient of variation for the inter-spike intervals greater than 50% were excluded from the analysis. The exclusion criterion was included to remove mixed clustered motor unit spike trains. However, this phenomenon happened only occasionally, since the second iterative procedure (figure 4) and the final sorting were implemented to favor the most regular estimations. Additionally, for all motor units identified in the results reported in table 2, we calculated the decomposability index (DI) as described by Florestal *et al* (Florestal *et al* 2009). Briefly, the DI index quantifies the difficulty of the decomposition according to the similarity of the identified MUAP shapes.

Note that equation (7) assumes that the two decompositions are totally independent, which is approximately valid in the cases analyzed. It is also noted that the accuracy is likely greater than that estimated with the RoA since a discrepancy in the decomposition may be due to an error in only one of the decompositions while it is considered a mistake for both.

The two source method was applied in this study to (1) two multi-channel intramuscular recordings obtained from the same muscle concurrently (decomposed either manually and automatically by the proposed approach); and (2) multi-channel intramuscular and multi-channel surface EMG recordings obtained concurrently (decomposed automatically by the proposed approach).

Experimental signals: intramuscular multi-channel thin-film recordings

Multi-channel intramuscular recordings were obtained with novel thin-film electrode systems designed for acute human recordings (Muceli *et al* 2015). The structure of the electrodes contains a linear array of 16 platinum detection points (140 μm $\times$ 40 μm) with 1 mm inter-electrode distance. The detailed description of the characteristics of the thin-film electrode used in this study can be found in (Muceli *et al* 2015).

Four men participated in the experiments (age 33 $\pm$ 6 years) that involved measures from the abductor digiti minimi (ADM, one participant), the first dorsal interosseous (FDI, one participant), and the tibialis anterior (TA, two participants) muscles. Some of the data have been obtained in an experiment to validate the thin-film electrodes (Muceli *et al* 2015). The experimental procedures were approved by the Ethics Committee of the University Medical Center Göttingen and conducted according to the Declaration of Helsinki, with an informed consent form signed by all participants before each experiment.

For the recordings performed from the ADM and FDI muscles, the hand of the participant was constrained in an instrumented brace that measures the exerted force of the muscle, similar to previous studies (Negro *et al* 2009, Negro and Farina 2011, 2012). The isometric abduction forces of the index and little finger were measured using a calibrated load cell (Interface, Scottsdale, AZ). One thin-film electrode was inserted into either the ADM or FDI muscle with an angle of approximately 30 or 60 degrees with respect to the skin surface. For the two experiments performed on the TA muscle, two thin-film electrodes were inserted into the muscle approximately 2 cm apart in the longitudinal direction. The subject was seated in a Biodex System 3 (Biodex Medical Systems Inc., NY, USA) with the right leg and foot fixed to the device. The target force profiles recorded in each experiment were the same for all muscles.

In all experiments, intramuscular EMG signals from the thin-film electrodes were recorded with a multi-channel amplifier (EMG-USB2, OT-Bioelettronica, Torino, Italy), band-pass filtered (100–4400 Hz), sampled at 10 000 Hz (ADM) or 10 240 Hz (FDI and TA), and A/D converted with 12 bits resolution. The EMG signals were acquired in bipolar derivation for the recordings performed on the ADM and FDI muscles, and in unipolar derivation for recordings from the TA muscle. A reference electrode was placed at the wrist (ADM and FDI) and the ankle (TA). In all experiments, the subjects were asked to perform a series of isometric contractions (abduction of the little finger for the ADM muscle, abduction of the index finger for the FDI muscle, and ankle dorsi-flexion for the TA muscle). The relative forces were determined in all cases as percentages of the maximal voluntary contraction (MVC) force, which was measured three times (the highest value was assumed as MVC). The relative contraction forces were 10% and 15% MVC for the ADM (duration 30-50 s), 10%, 20%, 30% for the TA (duration 50 s), and 10%, 50%, and 90% MVC for the FDI muscle (duration 20–30 s). A period of rest of 1 to 5 min was provided between contractions to prevent myoelectric fatigue. A visual feedback of the exerted force was provided to the subject.

For the validation based on comparison with an expert decomposition, the operator used the algorithm described in (McGill *et al* 2005) for assisted, semi-automatic decomposition. The decomposition was performed on each single channel individually by the expert operator and then the results were merged. The manual decomposition of each recording was performed on an average duration of 21 ± 13 s. In general, blind source separation approaches that relies on the maximization (or minimization) of cost functions should be applied to signals of lengths >10 s (Holobar and Zazula 2007b). The quality of the manual decompositions was assessed comparing the common motor unit spike trains identified in multiple channels and using the signal-to-interference ratio (SIR), as proposed by (Holobar *et al* 2010). In addition to the comparison with manual decomposition, the recordings with the two thin-film electrodes were used for the two source validation. Finally, the accuracy of intramuscular decomposition was also tested by the two source method applied between the intramuscular and surface EMG recordings (see below). In our analysis, we did not exclude channels with low signal-to-noise ratio from the EMG recordings. Occasionally, few iEMG channels showed higher levels of baseline noise, but, according to our results, this did not influence significantly the accuracy of the decomposition.

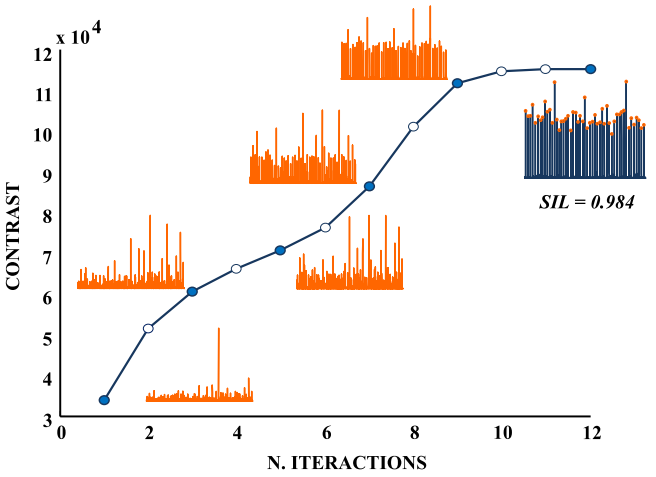

Figure 2. Representative example of the automatic identification of one motor unit spike train using the proposed algorithm (up to the first iteration cycle). At each iteration, a selected contrast function ($1/3x^3$ in this case) applied to the estimated source (estimation of non-gaussianity) is computed. The convergence is reached when the measure of non-gaussianity does not vary with respect to the previous iteration, up to a tolerance (*tolx*) that was fixed to 10^{-4} in this example. A peak detection approach and K-means classification is then applied for a first estimate of the instantaneous discharge pattern of the motor unit. The full method proposed in this study also includes a second iteration cycle, whose effect is not shown here.

Experimental signals: multi-channel surface EMG

A surface grid of 64 electrodes (5 × 13) (OT Bioelettronica, Torino, Italy) was placed after the insertion of the thin-film electrode for the experiment performed on the FDI muscle and for one subject on the TA muscle. The high-density grid of surface EMG electrodes with 4 mm (FDI) and 8 mm (TA) inter-electrode distances was positioned over (FDI) and beside (TA) the thin-film wire. The surface EMG signals were band-pass filtered (10–900 Hz), sampled at 10 240 Hz, and A/D converted to 12 bits. The EMG signals were recorded concurrently with the intramuscular EMG signals, during the contractions described above. The surface EMG decomposition was evaluated with the two source method that could be applied by comparing the concurrent automatic decompositions of the intramuscular and surface EMG. Prior to the application of the proposed decomposition algorithm, the sEMG signals were down-sampled to 2048 Hz. For the FDI muscle only, the surface matrix was slightly bigger than the recorded muscle. Therefore, we excluded the channels that did not show significant EMG activity by visual inspection (approximately 10 channels in each recording).

The average discharge rates and coefficients of variation of inter-spike intervals (ISI) ($SD_{ISI}/MEAN_{ISI}{}^{*}100$) reported in the tables were calculated by excluding abnormally long (>250 ms) or short (<20 ms) ISI values. The values of coefficients of variation of inter-spike intervals used for the second iteration of the proposed algorithm were calculated without excluding any value. We checked the normality of the discharge rates and the coefficients of variation of inter-spike intervals using the one-sample Kolmogorov-Smirnov test. The test showed that the values of coefficients of variation of inter-spike intervals were not normally distributed, therefore the Sign test with significance level $P < 0.05$ was used to test for statistical differences.

Results

We show the results of the decomposition performed with the proposed approach on intramuscular (15 or 32 channels) and surface (64 channels) EMG signals. First, we justify the selection of the extension parameter, the orthogonalization approach, and the second iteration following the fastICA (see Step 5 in the pseudocode). Second, we provide a set of results proving the accuracy of the proposed decomposition method.

Figure 2 shows a representative example of the estimation of one motor unit pulse train using the fixed point algorithm (see Methods). The non-linear contrast function used in this example was $G(x) = 1/3x^3$. The initial projection vector was set to an instant of time with high motor unit activity. In this example, the convergence (tolerance *tolx* set to 10^{-4}) was reached after 12 iterations. SIL as calculated after the convergence was equal to 0.98.

For all decompositions performed in this study, we selected the extension parameter equal to $1000/m$, where m was the number of channels of the recording. We tested different values of the extension parameter (from 2 to 64 for iEMGs and from 8 to 31 for sEMGs), but the results were not substantially influenced by the value of this parameter in these ranges. Table 1 shows an example of this analysis performed on one representative signal (Subject I, TA muscle, 30% MVC). Accuracy was not substantially different whereas the number of identified motor units increased with the extension

Table 1. Decomposition accuracy with different extension factors: thin-film (automatic).

Extension Factor	No. MUs	No. MUs (common)	RoA [%]
2	6	6	96.3 ± 1.9 (91.5–99.6)
4	11	11	91.8 ± 13.0 (67.0–99.6)
8	16	15	96.6 ± 4.2 (85.3–99.6)
16	20	18	93.5 ± 10.7 (61.3–99.6)
32	22	20	94.7 ± 6.7 (75.7–100.0)
64	19	19	96.0 ± 6.6 (70.8–99.6)

RoA: Rate of Agreement (mean ± SD, min-max); MU: Motor Unit.

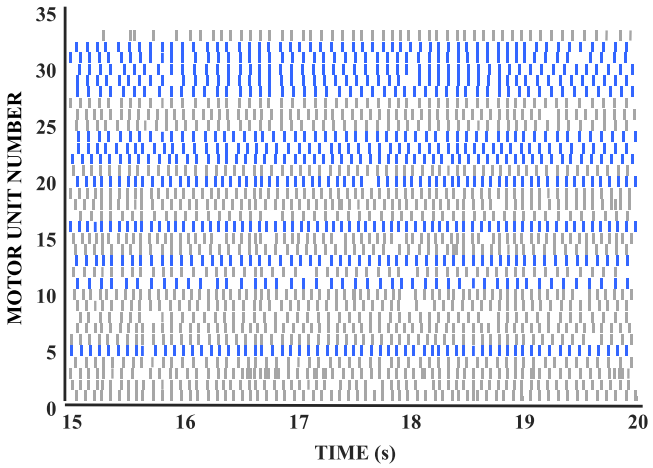

Figure 3. Representative example of the application of the Gram–Schmidt orthogonalization procedure used to increase the number of estimated sources. The same surface EMG signal (muscle TA, contraction force 20% MVC) was decomposed without (13 motor unit spike trains extracted, blue spikes) and with the proposed orthogonalization (all 33 spike trains shown; the gray spikes are those extracted only with orthogonalization). With orthogonalization, a total of 33 sources, of which 13 corresponding to those extracted without orthogonalization, were extracted.

factor, but reached the plateau region for extension factors higher than 16.

One of the major limitations of iterative blind source separation approaches is the repeated convergence to the same source. To overcome this problem, we implemented a deflation approach with orthogonalization and, contrary to (Chen and Zhou 2015) (see Methods), without peel-off procedure. Figure 3 shows an example of decomposition of a set of surface EMG signals with and without the orthogonalization step. In the first case, the algorithm with $M = 100$ repetitions of the 'for' loop (see the pseudocode) could extract only 13 unique sources since it iterated often on the same source. With the orthogonalization step and all other conditions similar, in the same example, the algorithm extracted 33 unique sources. Of these extracted sources, 13 were the same motor unit spike trains extracted without the orthogonalization (blue lines in figure 3) and 20 were the additional units (grey lines in figure 3). The trend shown in this representative result was confirmed in all cases.

The second iteration (Holobar and Zazula 2007b) was added to improve the source estimation performed with the fixed point algorithm. Figure 4 shows an example of the effect of this second iteration applied to one source extracted from a thin-film intramuscular recording. For this source, we provide the estimated accuracy by the RoA with reference to the manual decomposition. After the convergence of the fixed point algorithm (first iteration), in this representative example, the estimated innervation pulse train contained numerous errors as indicated by a value of the RoA of only 80.5%. The coefficient of variation of the inter-spike interval was $CoV_{ISI} = 44.2\%$ (figure 4(A)). Following a new calculation of the projection vector (step 5 in the pseudocode, see Methods), the number of errors in the innervation pulse train was substantially reduced so that the RoA reached 99.2%. Concurrently, the CoV_{ISI} decreased to 14.7%, showing that the high variability at the end of the first iteration was due to decomposition errors (figure 4(B)).

With one last iteration, this source could be extracted with RoA of 100%, to which corresponded a CoV_{ISI} of 13.3%. Further iterations did not change the CoV_{ISI} and therefore the process was stopped after only three iterations in this case. It is important to note that the presented RoA is available in this example exclusively because we performed the manual decomposition and applied the two source method for validation. In other conditions, RoA would not be available. However, the iterations shown were not based on any information on the RoA, but exclusively on the estimated value for CoV_{ISI}. The process was iterated until CoV_{ISI} did not change anymore and this corresponded to an increase in accuracy from a relatively low 80.5% to 100%. Similar behavior was observed in all other decompositions. The second iteration, absent in previous approaches based on fastICA (Ning *et al* 2014), thus significantly increases the performance of fastICA decomposition.

The accuracy of the manual decomposition by an expert was very high. This was proven by comparing the common motor unit discharge patterns when the expert decomposed the signals from the two distinct thin-film multichannel recordings in the TA muscle. For the full set of motor units compared from the TA of one subjects ($N = 93$), the average RoA for the two manual decompositions by the expert was 98.5 ± 2.4%. Thus, the manual decomposition of intramuscular signals could be considered as a solid gold standard.

The average signal-to-interference (SIR) ratio for the manually decomposed signals was 74.8 ± 10.7%. Such large value guarantees that the manual decompositions were performed optimally, minimizing the residual part of the signals. The comparison of the manual decomposition with the one obtained automatically with the proposed fully automatic multi-channel decomposition algorithm for intramuscular signals was performed on a total of eight multichannel EMG recordings, two of the ADM muscle (10 and 15% MVC contractions) of one subject and six (10, 20 and 30% MVC contractions) of the TA muscle of the other two subjects. Table 2 shows the results of this comparison. The average number of motor unit discharge patters that were matched between the two decompositions (manual and automatic) was 18 ± 4, with a relatively high RoA (>91%) in all the cases (table 2). The relatively large discrepancy between the

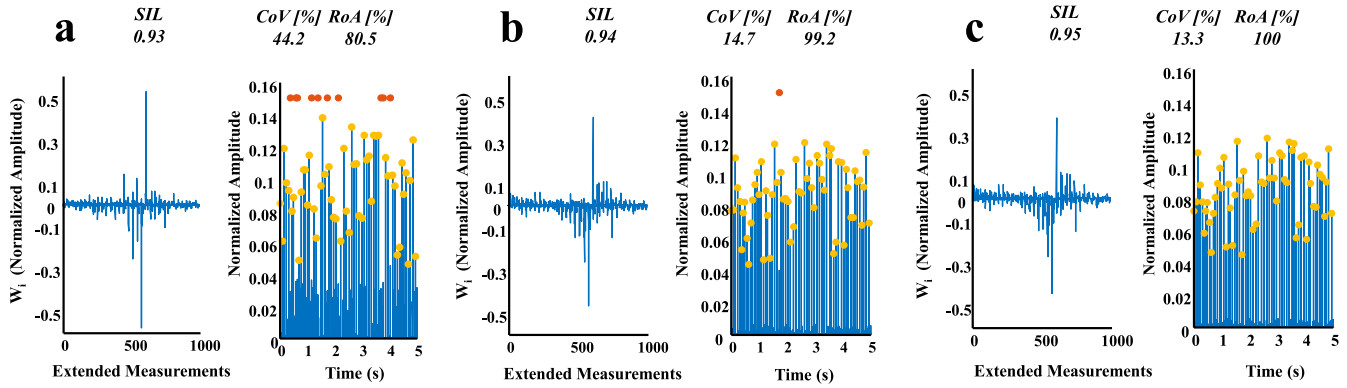

Figure 4. Example of the application of the second iterative procedure for improving the source estimation accuracy. At each iteration, the new projection vector (see step 5 in the pseudo code of the full algorithm in Methods) and the estimated innervation pulse train are shown. (A) Estimated discharge times (orange circles) extracted from the innervation pulse train at the last iteration of the fixed point algorithm. The comparison with the manual decomposition revealed several missed firings (red circles). (B) Estimated discharge times after the first iteration of the second iterative cycle. (C) Estimated discharge times at the last (third in this case) iteration of the second iterative cycle. The rate of agreement (RoA) for the extracted motor unit spike train improved from 80.5% to 100% with just three iterations.

number of motor units identified by the manual decomposition and the automatic one (second subject of TA muscle) is likely due to the fact that the automatic decomposition is biased to the identification of the sources with the highest energy. Accordingly, the average DI of the motor units identified by the manual decomposition were similar to the ones identified by the proposed method. Furthermore, we calculated the correlation between the RoA and the DI values and we found a relatively weak significant correlation ($R^2 = 0.34$, $P < 0.001$, Spearman test).

Table 3 shows the averaged discharge rates and the coefficients of variation for inter-spike intervals of the motor units identified by both manual and automatic decomposition. There were no statistical differences between these variables characterizing motor unit behavior in all the cases, with the exception of the CoV for the inter-spike interval of the TA motor units at 30% MVC (one subject). For these eight multichannel EMG signals, the SIL measure was strongly positively associated to the RoA for all motor units, with a slope of 0.98 (linear least square regression with intercept equal to zero). Therefore, the SIL measure is a practical estimate of the RoA when the two sources comparison is not available. Contrary to the PNR, which is non-linearly associated to RoA (Holobar *et al* 2014), the SIL measure proposed in this study is normalized and thus maps directly to RoA.

Figure 5 shows an example of the two source comparison (manual versus automatic decomposition) for intramuscular signals and the effect of decomposition errors on the instantaneous discharge rate of the extracted motor units. In this example, 17 motor units were matched and compared between the two decompositions (circle: automatic decomposition; cross: manual decomposition). The mismatches, which determine differences in the instantaneous discharge rates, are shown in red. When the signals from the two thin-film wires in the TA muscle were decomposed independently using the proposed algorithm (two source method with automatic decomposition of two multi-channel intramuscular signals), the average RoA was 95.2 ± 10.6% (N = 33) for 6 trials of the TA recorded from two subjects at 10%, 20% and 30% MVC.

The two source method was then applied between intramuscular and surface EMG decompositions. Concurrent recordings in this case were performed on the TA (one subject) and FDI (one subject) muscles. In this case, the validation consisted in the comparison of decompositions of the intramuscular and surface recordings using the proposed automatic algorithm. Table 4 shows the averaged results for three contraction forces (10%, 50% and 90% MVC) in the FDI of one subject. In the TA muscle, there were no common motor units detected and therefore the RoA could not be computed. Table 5 shows the averaged discharge rates and the coefficients of variation for inter-spike intervals for the same common units. There were no significant differences between these variables when obtained from the two decompositions. Figure 6 shows an example of surface versus intramuscular validation performed at 90% MVC in the FDI muscle. In this case, the average rate of agreement was >90%.

The concurrent recording of intramuscular and surface EMG signals provided the possibility not only of validating the decompositions, but also of identifying a relatively large number of motor units. In this study, we extracted from both signals an average of 57 ± 4 unique motor units for the TA muscle and 16 ± 2 unique motor units for the FDI. Figure 7 shows an example of the decomposition performed on the TA muscle in one subject using both intramuscular and surface recording systems concurrently. In this example, 59 unique motor units were identified from the two recordings and their discharge patterns were estimated in a fully automatic way. In addition to the discharge timings, on which we have focused so far, it is also possible to extract the shape of the multi-channel action potentials (3D for surface recordings and 2D for intramuscular recordings) by spike triggered averaging (Holobar *et al* 2009).

Figure 8 shows a representative example of surface motor unit action potential in the two spatial dimensions and in time. The temporal waveform of the motor unit is shown for each

Table 2. Decomposition Accuracy for the intramuscular thin-film signals: Manual versus Automatic decomposition.

Contraction Level [%MVC]		No. MUs (manual)	No. MUs (automatic)	No. MUs common	RoA (%)	DI (manual)	DI (automatic)
ADM 15 *ch*	10	23	14	14	91.8 ± 9.2 (60.6–98.7)	14.6 ± 11.6 (7.6–63.4)	15.8 ± 7.4 (10.0–35.7)
	15	31	14	14	91.5 ± 6.6 (75.7–99.2)	11.9 ± 6.3 (6.5–34.0)	12.2 ± 5.3 (7.9–27.4)
TA 2 × 16 *ch*	10	14	14	13	97.0 ± 7.0 (77.5–100.0)	21.6 ± 10.5 (6.3–46.7)	22.2 ± 10.2 (10.8–44.1)
	20	20	17	17	97.5 ± 4.5 (84.6–99.8)	21.0 ± 14.7 (7.7–76.6)	20.5 ± 6.9 (11.7–38.3)
	30	27	22	20	95.9 ± 3.4 (88.3–99.6)	14.4 ± 6.2 (6.7–39.4)	16.7 ± 6.7 (9.7–40.7)
TA 2 × 16 *ch*	10	53	22	22	95.6 ± 8.66 (58.9–99.1)	14.9 ± 4.7 (9.5–35.5)	16.7 ± 4.4 (9.5–28.3)
	20	57	24	24	93.9 ± 11.5 (45.0–99.3)	11.1 ± 2.3 (7.7–17.4)	12.3 ± 2.2 (7.3–17.0)
	30	60	21	21	93.4 ± 9.6 (55.7–100.0)	10.4 ± 2.1 (7.0–17.9)	11.9 ± 2.4 (8.4–17.7)

ADM: Abductor Digiti Minimi; TA: Tibialis Anterior; RoA: Rate of Agreement (mean ± SD, min-max); DI: Decomposability Index (mean ± SD, min-max) ch: channels.

Table 3. Statistics of motor unit behavior for the decompositions of the intramuscular thin-film signals: Manual versus Automatic decomposition.

Contraction Level [%MVC]		Mean DR [pps] (manual)	Mean DR [pps] (autom.)	CoV ISI [%] (manual)	CoV ISI [%] (autom.)
ADM	10	15.2 ± 4.3	15.6 ± 4.3	26.3 ± 5.9	23.1 ± 7.4
	15	14.8 ± 4.8	15.0 ± 4.6	22.1 ± 4.3	24.3 ± 4.4
TA	10	11.2 ± 1.0	11.7 ± 1.9	12.8 ± 2.8	14.4 ± 5.9
	20	11.6 ± 1.1	11.7 ± 1.2	13.7 ± 4.7	15.7 ± 5.6
	30	12.6 ± 1.1	12.6 ± 1.1	14.9 ± 3.4	16.7 ± 5.2
TA	10	9.8 ± 1.5	10.3 ± 2.8	13.9 ± 3.7	16.4 ± 7.0
	20	12.8 ± 1.2	13.3 ± 2.4	12.1 ± 5.2	14.7 ± 8.0
	30	13.7 ± 2.0	14.1 ± 2.7	**12.9 ± 3.1***	**17.6 ± 7.1***

*, $P < 0.05$.
ADM: Abductor Digiti Minimi; TA: Tibialis Anterior; CoV: coefficient of variation; ISI: inter-spike interval; DR: discharge rate, and pps: pulses per second. The data are averaged across the number of MUs that were identified with manual and automatic decomposition, respectively.

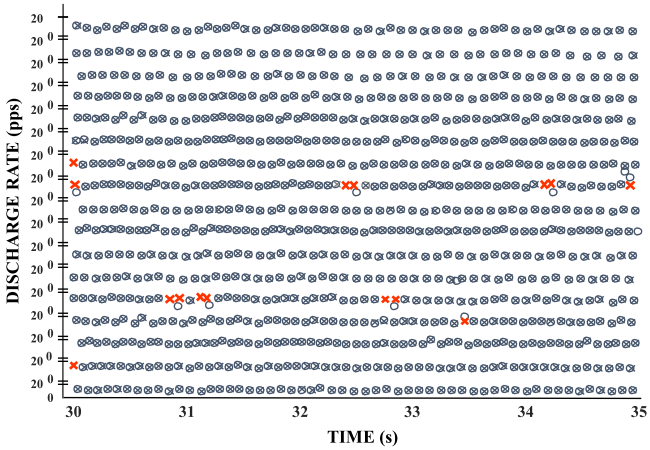

Figure 5. Example of validation performed on one set of thin-film EMG signals recorded from the TA muscle decomposed manually and automatically with the proposed method. For each extracted motor unit spike train, the instantaneous discharge rate is shown for the automatic decomposition (circles) and the manual decomposition (crosses). The mismatches are in red. pps: pulses per second.

channel (top) with the 2D spatial representations for three instants of time (20, 25 and 30 ms) (bottom). In a reliable decomposition, the action potentials of each motor unit should be unique (Farina *et al* 2008a). Figure 9 shows an example of the spatial representations of 9 surface motor unit action potentials extracted during one of the contractions of the TA muscle, at a fixed instant of time. These motor units have a unique signature. Figure 10 shows a similar example for the representation of motor unit action potentials extracted from the intramuscular thin-film electrode. In this case, the representations are spatio-temporal (15 electrodes × 20 ms) and show six unique action potential shapes that evolve in space and time.

Discussion

This study proposes a framework for the decomposition of multi-channel intramuscular and surface EMG signals adapted from the general convolutive blind source separation approach presented originally in (Thomas *et al* 2006). The framework includes the approaches presented by (Holobar and Zazula 2007b) and (Chen and Zhou 2015) for surface EMG decomposition. For the first time, we apply blind source separation methods to multi-channel intramuscular EMG signals, for a complete automatic decomposition. Moreover, we provide an extensive validation of the proposed decomposition framework for both intramuscular and surface EMG decomposition, which is conversely missing in some previous studies (Chen and Zhou 2015).

The proposed method includes a convolutive sphering (extension and whitening) of the measurement matrix, followed by an iterative optimization of separation vectors that aims at maximizing the non-gaussianity and, thus, the sparseness of the extracted sources. This approach, which is a combination of the fastICA and CKC decomposition algorithms, with some modifications to make it suitable to both intramuscular and surface EMG decomposition, is possible because of specific properties of the discharge patterns of motor units which have been detailed above.

In order to increase the separability of a convolutive mixture, the number of extended measurements should be larger than the product between the number of sources and the length of the MUAP in samples. For surface EMG signals sampled at 2 k Hz, the extension factor is typically set to $R = 10$ (Holobar and Zazula 2007b). In the proposed study, we compared the performance of the algorithm for different extension factors and we confirmed that the extension factors should be larger than 16 for iEMG signals sampled at 10 k Hz (table 1). In general, the MUAP duration is influenced by the inter-electrode distance, the size of the electrodes and the location (intramuscular or superficial). Therefore, dense matrices with small electrodes and short inter-electrode distances should be preferable for the proposed technique.

The resulting extended sources are uncorrelated for time lag zero (needed in our approach for the whitening step) if the autocorrelation function of each source is approximately zero for time lags in the range 1 up to the sum of the length of the filters in the convolutive mixture and the degree of extension of the observations ($L + R - 1$). For Gaussian distributed inter-spike intervals, this condition is never verified exactly, but it is well approximated if $L + R$ is smaller than the minimum average inter-spike interval among the estimated

Table 4. Decomposition Accuracy for the proposed algorithm: Thin-Film versus Surface decomposition (automatic).

Contraction Level [%MVC]		No. MUs (thin-film)	No. MUs (surface)	No. MUs common	RoA [%]
FDI	10	12	15	6	97.6 ± 2.6 (91.9–99.6)
	50	9	16	4	91.1 ± 7.3 (70.0–97.9)
	90	8	12	6	91.0 ± 2.2 (88.1–94.3)

FDI: First Dorsal Interosseus; RoA: Rate of Agreement (mean ± SD, min-max)

Table 5. Statistics of motor unit behavior for the decompositions: Thin-Film versus Surface decomposition (automatic).

Contraction Level [%MVC]		Mean DR (thin-film) [pps]	Mean DR (surface) [pps]	CoV ISI (thin-film) [%]	CoV ISI (surface) [%]
FDI	10	14.2 ± 2.6	13.4 ± 1.1	19.0 ± 2.3	20.1 ± 3.2
	50	19.1 ± 4.1	19.7 ± 3.5	40.2 ± 5.6	39.8 ± 6.6
	90	26.9 ± 1.9	27.2 ± 1.8	41.7 ± 8.4	41.5 ± 9.0

FDI: First Dorsal Interosseus; CoV: coefficient of variation; ISI: inter-spike interval;
DR: discharge rate, and pps: pulses per second.

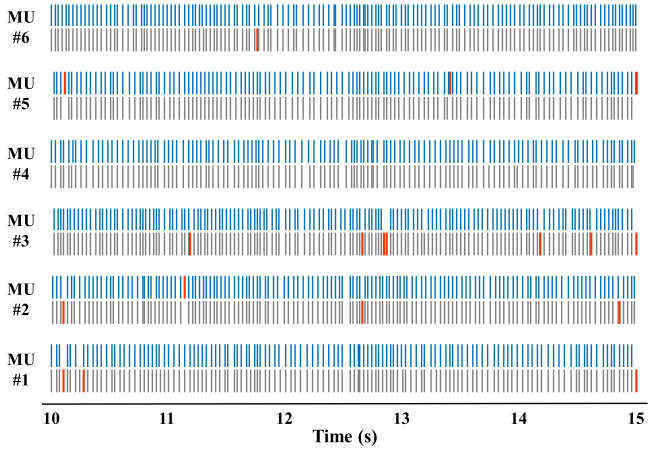

Figure 6. Validation of the decomposition results using the proposed automatic method on two concurrently recorded EMG signals (thin-film and surface) on the FDI muscle at 90% MVC. The comparison is reported for 6 motor units identified by both the decomposition of the thin-film signals (grey spikes) and of the surface signals (blue spikes) for a representative interval of 5 s duration. Mismatches are shown in red. In this example, the RoA calculated for the entire recording of durations 30 s was 91.0 ± 2.2%. MU: Motor Unit.

sources and if the variability is small (see appendix) (Holobar and Zazula 2007b).

In addition, we revealed why the extension of sources, required by the transformation of the convolutive data model to the instantaneous one, does not hinder the decomposition approaches designed for separation of independent sources, even though the extended sources are never independent. Namely, the contrast functions used for measuring the independence frequently also estimate the sparseness of sources. A linear mixture of two differently delayed versions of the same pulse train is always less sparse than the original pulse train. Therefore, the contrast functions used in this application (decomposition of EMG signals) do not measure independency, as claimed in (Chen and Zhou 2015), but rather sparseness of motor unit spike trains. Moreover, sparseness is a function of the discharge rate: the greater the discharge rates, the lower the sparseness of the sources. In physiological conditions, the refractory period of human motor neurons provides a lower bound to the minimum inter-spike interval (discharge rates of 30–40 pps), satisfying the sparseness assumption quite well. Even the occurrence of physiological or pathological doublets (>50 pps) presents no challenges to the algorithm as similar approaches have been previously applied to signals recorded during pathological tremor with excellent results (Holobar *et al* 2012).

One of the main limitations in the source separation techniques is the repeated convergence to the same source. To overcome this problem several methods have been proposed in the signal processing literature (Thomas *et al* 1990, Hyvärinen and Oja 2000). Contrary to the subtraction of the estimated sources from the observations (peel-off), implemented, e.g., in (Chen and Zhou 2015), we applied source deflation that projects the updated separation vector in the orthogonal space of the previously estimated vectors (Hyvärinen and Oja 2000). The technique demonstrated the ability to increase the number of the extracted units (figure 3). A similar approach can be applied in parallel using symmetric orthogonalization (Hyvarinen 1999, Hyvärinen and Oja 2000, Chen and Zhou 2015), however, in this study, this was computationally not feasible, at least for intramuscular EMG signals because of their relatively high sampling rate.

In addition to the fixed point iteration, we added a second iteration (similar to the CKC algorithm) to improve the source estimation (figure 4). This second iterative approach aims to remove spurious discharges by identifying a better estimation of the separation vector. It was assumed that this improved estimate would correspond to a decrease in the estimated inter-spike interval variability of the corresponding motor unit spike train. A similar procedure was applied to sorting the total number of estimated sources. This procedure favors the regularity in motor unit discharges, but does not enforce it (Holobar *et al* 2010, Holobar *et al* 2014). The representative example of figure 4 shows the extreme efficacy of the proposed iterative estimation of the ideal projection vector (note the substantial decrease in the baseline noise even after a few

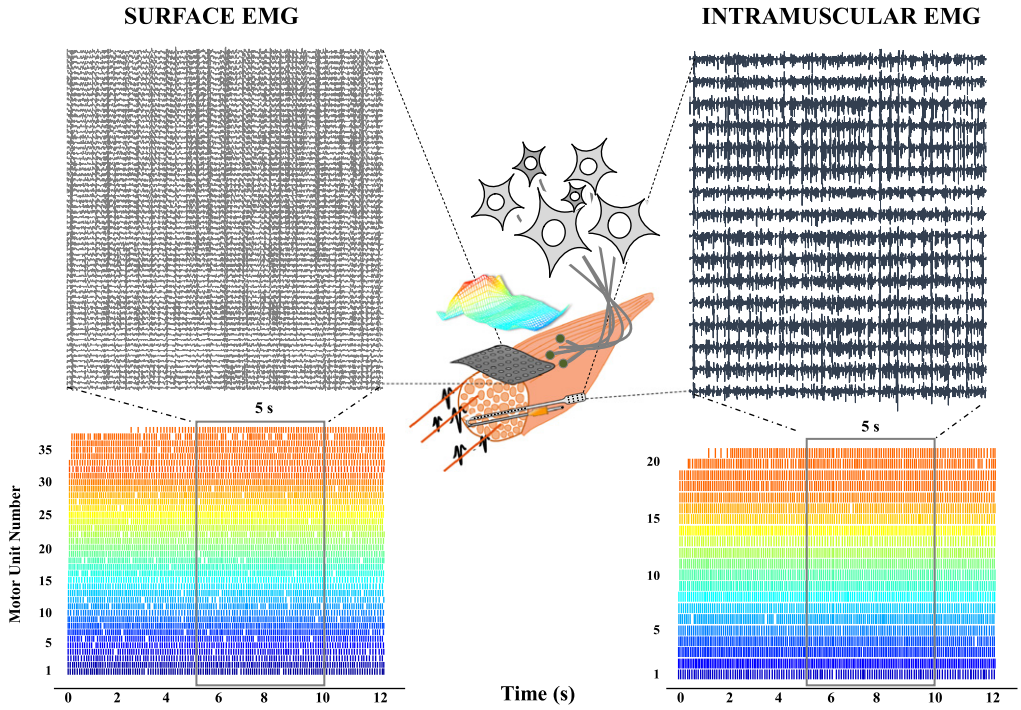

Figure 7. Example of automatic concurrent decomposition of thin-film and surface EMG signals from the tibialis anterior muscle during a contraction at 30% MVC. Only 16 intramuscular channels are shown for clarity, although 32 were used for the decomposition. The total number of unique motor units decomposed was 59.

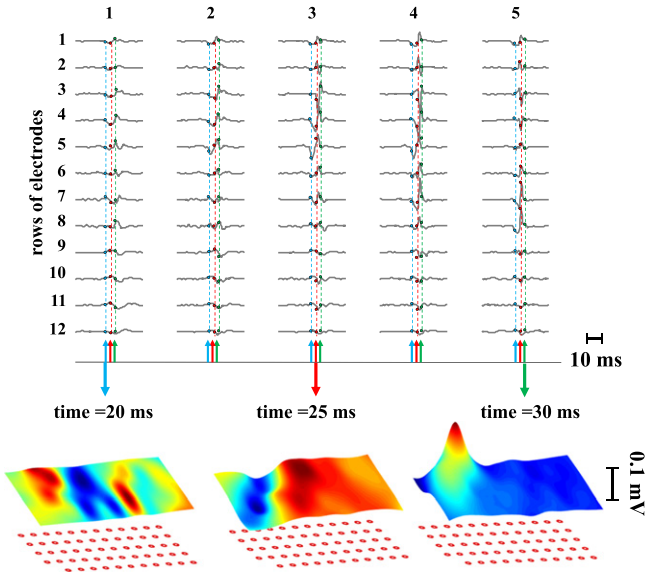

Figure 8. Motor unit action potential obtained by spike averaging using the decomposed multi-channel surface EMG signals to derive the trigger. The spike triggered waveforms are shown for each electrode and the 2D spatial representation is shown for three time instants (20, 25 and 30 ms). Muscle TA, contraction force 20% MVC.

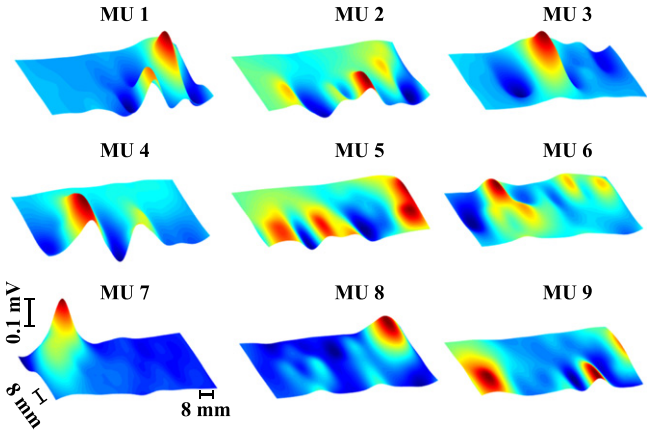

Figure 9. Spatial representation of multiple motor units extracted from surface EMG decomposition from a contraction at 20% MVC of the TA muscle. Nine unique motor unit action potentials recorded from a surface grid of 13 × 5 electrodes are shown. MU: Motor unit.

iterations). The second iterative process may be applied to both steady and variable contraction forces. In fact, the main assumption of the method is that the superimposition of two motor unit spike trains is always more variable that the single ones. In normal condition, this assumption is reasonable for both steady and variable discharge rates. However, it may happen that the method will fail in extreme situations (pathological conditions, afferent stimulation or vibration) and further analyses will need to be performed in the future. However, it is worth noting that the proposed method does not necessarily need to be applied with the constraint of decreasing the coefficient of variation of the inter-spike interval. Any other criteria for stopping the second iteration would also be acceptable. For example, it would be possible to apply the SIL measure to this second iteration (note that this measure would also increase with the number of iterations, being an efficient criterion for determining

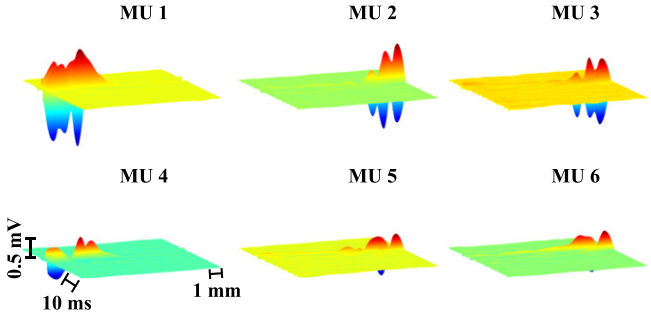

Figure 10. Spatio-temporal representation of motor unit action potentials obtained from the decomposition of intramuscular thin-film signals during a contraction at 20% MVC of the TA muscle. Six unique motor unit action potentials, functions of space and time, are shown (15 channels × 20 ms). MU: Motor Unit.

convergence). In this example, the variability of the inter-spike interval would not be minimized and therefore no constraints would be imposed on the statistics of the estimated motor unit discharges.

One of the fundamental issues in the development of EMG decomposition algorithms is their proper validation (De Luca *et al* 2006, Farina and Enoka 2011, Farina *et al* 2014, 2015, De Luca *et al* 2015). In this study, the proposed framework was extensively validated with state of the art approaches on experimental signals. For this purpose, intramuscular EMG decompositions (both manual and automatic) of different intramuscular signals with some common sources have been compared (figure 5 and tables 2 and 3). Moreover, the same intramuscular decomposition was compared with concurrently recorded and decomposed surface EMG signals (figure 6 and tables 4 and 5). In all cases, the RoA between the estimations of the common sources has been used as a conservative measure of accuracy. This approach is superior to those limited to only simulated conditions (Chen and Zhou 2015), as well as to several indirect methods that have been shown to have important limitations (Farina *et al* 2014, Hu *et al* 2014, Kline and De Luca 2014). Moreover, contrary to the two source method applied only as a comparison between intramuscular and surface EMG decomposition (Holobar *et al* 2010, Marateb *et al* 2011a, Holobar *et al* 2014), we could also estimate the accuracy of the expert decomposition by comparing the same sources identified on two different thin-film electrodes by the expert. Note that the two source method is only appropriate when the two EMG recording modalities compared differ significantly in the shapes of recorded motor unit action potentials. This condition is usually well met when comparing two intramuscular sets of EMG signals (Mambrito and De Luca 1984, McGill and Marateb 2011) or intramuscular and surface EMG signals. However, this cannot easily be claimed for two sets of surface EMG signals.

In addition to providing means for validation of accuracy, the decomposition of concurrently recorded multi-channel intramuscular and surface EMG signals offers the possibility to increase the number of unique motor unit spike trains that can be identified during voluntary contractions in humans (figure 7). In this study, applying the proposed framework to concurrent intramuscular and surface EMG recordings, we extracted an average of 57 ± 4 unique motor units in the TA muscle (with one non-invasive grid and two thin-film electrodes) and 16 ± 2 in the FDI muscle (with a similar configuration, but only one thin-film electrode). These numbers are very high if we compare them with the number of motor unit spike trains extracted using traditional approaches (Merletti and Parker 2004, Merletti and Farina 2009) and if we consider that they have been obtained in a completely automatic way, with an accuracy in discharge timing estimates greater than 90%.

Conclusion

In conclusion, we proposed a decomposition framework for multi-channel intramuscular and surface EMG signals and detailed its theoretical bases. The proposed decomposition approach was systematically validated experimentally on both multi-channel surface and intramuscular EMG signals. The validation showed high accuracy of this approach in a variety of conditions. Within this validation effort, this study is also the first to report accurate, fully automatic decomposition of multi-channel intramuscular EMG signals using blind source separation techniques.

Acknowledgments

This work was supported by the European Research Council under the Advanced Grant DEMOVE (contract #267888) to DF and by Slovenian Research Agency (contract # L5-5550) to AH.

Appendix A

In general, the correlation matrix of the extended sources $\underline{\tilde{s}}(k)$ is block-diagonal:

$$\underline{\underline{R}}_{\tilde{s}\tilde{s}}(0) = \begin{bmatrix} \underline{\underline{R}}_{\tilde{s}_1\tilde{s}_1}(0) & 0 & 0 \\ 0 & \ddots & 0 \\ 0 & 0 & \underline{\underline{R}}_{\tilde{s}_n\tilde{s}_n}(0) \end{bmatrix} \quad \text{(A1)}$$

where $\underline{\underline{R}}_{\tilde{s}_i\tilde{s}_i}(0) = E\{\tilde{s}_i(k)\tilde{s}_i(k)^T\}$ is the autocorrelation matrix of the extended i-th source. The non-zero block-diagonal entries of $\underline{\underline{R}}_{\tilde{s}\tilde{s}}(0)$ are the values of the auto-correlation functions of the original sources for the time lags 0 to $L + R - 1$ and can be analytically determined, as done in the following.

The motor unit spike trains can be described as sums of Dirac delta functions with an averaged inter-discharge inverval T_i (in samples) and random jitters θ_i that are independent, discrete random variables, which are assumed to have the same probability density function $f_{\theta_i}(u) = q(u), \forall\, i$, where u are the discrete values (in samples) that the random variable assumes. This discrete time stochastic process has the

following autocorrelation function (Dideriksen *et al* 2012):

$$R_{s_i s_i}(k) = \frac{1}{T}\left[\delta(k) + \sum_{l\neq 0} R_q(k - lT_i)\right], \quad k = -T_i, \ldots, T_i \tag{A2}$$

under the assumption that the probability density function $q(u)$ is zero outside the interval $\left(-\frac{T_i}{2}, \frac{T_i}{2}\right)$ (this assumption in practice implies that the next spike cannot occur earlier than the previous one).

Interestingly, $R_{s_i s_i}(k)$ [equation (A2)] is approximately zero for a range of values of k from 1 to a maximum delay that depends on the average discharge rate and its variability [see equation (A2)]. The greater the discharge rate and its variability, the smaller the range of k values for which $R_{s_i s_i}$ is practically null. Since $R_{s_i s_i}(k)$ also represents the off-diagonal values of the autocorrelation matrix of the extended sources [equation (A1)], we obtain:

$$\underline{R}_{\bar{s}\bar{s}}(0) = \begin{bmatrix} \underline{R}_{s_1 s_1}(0) & \cdots & \underline{R}_{s_1 s_1}(L+R) & & 0 & \\ \vdots & \ddots & \vdots & \cdots & \vdots & \\ \underline{R}_{s_1 s_1}(L+R) & \cdots & \underline{R}_{s_1 s_1}(0) & \ddots & \underline{R}_{s_n s_n}(0) & \cdots & \underline{R}_{s_n s_n}(L+R) \\ & \vdots & & \cdots & \vdots & \ddots & \vdots \\ & 0 & & & \underline{R}_{s_n s_n}(L+R) & \cdots & \underline{R}_{s_n s_n}(0) \end{bmatrix} \tag{A3}$$

References

Adrian E D and Bronk D W 1929 The discharge of impulses in motor nerve fibres *The Journal of Physiology* **67** 9–151

Arthur D and Vassilvitskii S 2007 K-means++: the advantages of careful seeding *Proc. of the Eighteenth Annual ACM-SIAM Symp on Discrete algorithms Society for Industrial and Applied Mathematics* p 1027–35

Belouchrani A, Abed-Meraim K, Cardoso J-F and Moulines E 1997 A blind source separation technique using second-order statistics *Signal Processing, IEEE Transactions on* **45** 434–44

Belouchrani A and Amin M G 1998 Blind source separation based on time-frequency signal representations *Signal Processing, IEEE Transactions on* **46** 2888–97

Chen M and Zhou P 2016 A Novel Framework Based on FastICA for High Density Surface EMG Decomposition*IEEE Trans. Neural Systems and Rehabilitation Eng.* **24** 117–27

De Luca C J, Adam A, Wotiz R, Gilmore L D and Nawab S H 2006 Decomposition of surface EMG signals *J. Neurophysiology* **96** 1646–57

De Luca C J, Nawab S H and Kline J C 2015 Clarification of methods used to validate surface EMG *J. Appl. Physiol.* **118** 1085

Dideriksen J L, Negro F, Enoka R M and Farina D 2012 Motor unit recruitment strategies and muscle properties determine the influence of synaptic noise on force steadiness *J. Neurophysiology* **107** 3357–69

Enoka R M 2008 *Neuromechanics of Human Movement* (Human kinetics)

Farina D and Enoka R M 2011 Surface EMG decomposition requires an appropriate validation *J. Neurophysiology* **105** 981–2

Farina D and Holobar A 2015 Human-Machine interfacing by decoding the surface electromyogram [life sciences] *Signal Processing Magazine, IEEE* **32** 115–20

Farina D, Merletti R and Enoka R M 2014 The extraction of neural strategies from the surface EMG: an update *J. Appl. Physiol.* **117** 1215–30

Farina D, Merletti R and Enoka R M 2015 Reply to De Luca, Nawab, and Kline: the proposed method to validate surface EMG signal decomposition remains problematic *J. Appl. Physiol.* **118** 1085–85

Farina D and Negro F 2015 Common synaptic input to motor neurons, motor unit synchronization, and force control *Exercise and Sport Sciences Reviews* **43** 23–33

Farina D, Negro F, Gazzoni M and Enoka R M 2008a Detecting the unique representation of motor-unit action potentials in the surface electromyogram *J. Neurophysiology* **100** 1223–33

Farina D, Yoshida K, Stieglitz T and Koch K P 2008b Multichannel thin-film electrode for intramuscular electromyographic recordings *J. Appl. Physiol.* **104** 821–7

Florestal J, Mathieu P and McGill K 2009 Automatic decomposition of multichannel intramuscular EMG signals *J. Electromyography and Kinesiology* **19** 1–9

Florestal J R, Mathieu P A and Malanda A 2006 Automated decomposition of intramuscular electromyographic signals *Biomedical Engineering, IEEE Transactions on* **53** 832–9

Florestal J R, Mathieu P A and Plamondon R 2007 A genetic algorithm for the resolution of superimposed motor unit action potentials *Biomedical Engineering, IEEE Transactions on* **54** 2163–71

Ge D, Le Carpentier E and Farina D 2010 Unsupervised Bayesian decomposition of multiunit EMG recordings using Tabu search *Biomedical Engineering, IEEE Transactions on* **57** 561–71

Ge D, Le Carpentier E, Idier J and Farina D 2011 Spike sorting by stochastic simulation *Neural Systems and Rehabilitation Engineering, IEEE Transactions on* **19** 249–59

Heckman C and Enoka R M 2012 Motor unit *Comprehensive Physiology*

Heckman C and Enoka R M 2004 Physiology of the motor neuron and the motor unit *Handbook of Clinical Neurophysiology* **4** 119–47

Holobar A and Farina D 2014 Blind source identification from the multichannel surface electromyogram *Physiol. Meas.* **35** R143

Holobar A, Farina D, Gazzoni M, Merletti R and Zazula D 2009 Estimating motor unit discharge patterns from high-density surface electromyogram *Clinical Neurophysiology* **120** 551–62

Holobar A, Glaser V, Gallego J, Dideriksen J L and Farina D 2012 Non-invasive characterization of motor unit behaviour in pathological tremor *J. Neural Eng.* **9** 056011

Holobar A, Minetto M and Farina D 2014 Accurate identification of motor unit discharge patterns from high-density surface EMG and validation with a novel signal-based performance metric *Journal of Neural Engineering* **11** 016008

Holobar A, Minetto M A, Botter A, Negro F and Farina D 2010 Experimental analysis of accuracy in the identification of motor unit spike trains from high-density surface EMG *Neural Systems and Rehabilitation Engineering, IEEE Transactions on* **18** 221–9

Holobar A and Zazula D 2007a Gradient convolution kernel compensation applied to surface electromyograms *Independent Component Analysis and Signal Separation* (Springer) p 617–24

Holobar A and Zazula D 2007b Multichannel blind source separation using convolution kernel compensation *Signal Processing, IEEE Transactions on* **55** 4487–96

Hu X, Rymer W Z and Suresh N L 2014 Accuracy assessment of a surface electromyogram decomposition system in human first dorsal interosseus muscle *J. Neural Eng.* **11** 026007

Hyvarinen A 1999 Fast and robust fixed-point algorithms for independent component analysis *Neural Networks, IEEE Transactions on* **10** 626–34

Hyvärinen A and Oja E 1997 A fast fixed-point algorithm for independent component analysis *Neural Comput.* **9** 1483–92

Hyvärinen A and Oja E 2000 Independent component analysis: algorithms and applications *Neural Netw.* **13** 411–30

Kline J C and De Luca C J 2014 Error reduction in EMG signal decomposition *J. Neurophysiology* **112** 2718–28

Liu Y, Ning Y, He J, Li S, Zhou P and Zhang Y 2014 Internal muscle activity imaging from multi-channel surface EMG recordings: a validation study *Engineering in Medicine and Biology Society (EMBC), 2014 36th Annual Int. Conf. of the IEEE* (IEEE) p 3559–61

Mambrito B and De Luca C J 1984 A technique for the detection, decomposition and analysis of the EMG signal *Electroencephalogr. Clin. Neurophysiol.* **58** 175–88

Marateb H R, McGill K C, Holobar A, Lateva Z C, Mansourian M and Merletti R 2011a Accuracy assessment of CKC high-density surface EMG decomposition in biceps femoris muscle *J. Neural Eng.* **8** 066002

Marateb H R, Muceli S, McGill K C, Merletti R and Farina D 2011b Robust decomposition of single-channel intramuscular EMG signals at low force levels *J. Neural Eng.* **8** 066015

McGill K C, Lateva Z C and Marateb H R 2005 EMGLAB: an interactive EMG decomposition program *J. Neurosci. Methods* **149** 121–33

McGill K C and Marateb H R 2011 Rigorous a posteriori assessment of accuracy in EMG decomposition *Neural Systems and Rehabilitation Engineering, IEEE Transactions on* **19** 54–63

Merletti R and Farina D 2009 Analysis of intramuscular electromyogram signals *Philosophical Transactions of the Royal Society A: Mathematical, Physical and Engineering Sciences* **367** 357–68

Merletti R and Parker P A 2004 *Electromyography: Physiology, Engineering, and non-invasive Applications* (John Wiley & Sons)

Mitianoudis N, Stathaki T and Davies M 2005 Blind separation of skewed signals in instantaneous mixtures *Signal Processing Systems Design and Implementation, 2005 IEEE Workshop on* (IEEE) p 407–12

Monsifrot J, Le Carpentier E, Farina D and Aoustin Y 2011 Sequential estimation of intramuscular EMG model parameters for prosthesis control *IEEE/RSJ Int. Conf. on Intelligent Robots and Systems, Workshop on Robotics for Neurology and Rehabilitation*

Muceli S, Poppendieck W, Negro F, Yoshida K, Hoffmann K P, Butler J E, Gandevia S C and Farina D 2015 Accurate and representative decoding of the neural drive to muscles in humans with multi-channel intramuscular thin-film electrodes *J. Physiology* **593** 3789–804

Nawab S H, Wotiz R P and De Luca C J 2008 Decomposition of indwelling EMG signals *J. Appl. Physiol.* **105** 700–10

Negro F and Farina D 2012 Factors influencing the estimates of correlation between motor unit activities in humans *PLoS One* **7** e44894

Negro F and Farina D 2011 Linear transmission of cortical oscillations to the neural drive to muscles is mediated by common projections to populations of motoneurons in humans *J. Physiology* **589** 629–37

Negro F, Holobar A and Farina D 2009 Fluctuations in isometric muscle force can be described by one linear projection of low-frequency components of motor unit discharge rates *J. Physiology* **587** 5925–38

Ning Y, Zhu X, Zhu S and Zhang Y 2015 Surface EMG Decomposition based on K-means clustering and Convolution Kernel Compensation *IEEE J. Biomed Health Inform* **19** 471–7

Ollila E 2010 The deflation-based FastICA estimator: statistical analysis revisited *Signal Processing, IEEE Transactions on* **58** 1527–41

Thomas C, Bigland-Ritchie B, Westling G and Johansson R 1990 A comparison of human thenar motor-unit properties studied by intraneural motor-axon stimulation and spike-triggered averaging *J. Neurophysiology* **64** 1347–51

Thomas J, Deville Y and Hosseini S 2006 Time-domain fast fixed-point algorithms for convolutive ICA *Signal Processing Letters, IEEE* **13** 228–31

Wei T 2014 On the spurious solutions of the Fastica algorithm *Statistical Signal Processing (SSP), 2014 IEEE Workshop on* (IEEE) p 161–4